

STUDY ON VIBRATION ANALYSIS METHODS FOR FLUID-STRUCTURE INTERACTION OF LMFBR STRUCTURE - FLOW HOLE TESTS

H. Katayama¹, K. Yamamoto², T. Funada², Y. Eguchi², S. Moriya³, S. Fujimoto¹ and T. Iijima⁴

¹Toshiba Corporation, Kawasaki, ²The Japan Atomic Power Company, Tokyo, ³Central Research Institute of Electric Power Industry, Abiko, ⁴Toshiba Corporation, Yokohama (Japan)

ABSTRACT

A large amount of liquid sodium in LMFBR reactor vessels is divided into two domains by a core support structure. These domains are connected by small flow holes in the core support structure. As a result, the bottom of the reactor vessel and the core support structure have two resonant coupling vibration modes caused by fluid-structure interaction in the vertical direction.

This paper deals with an experimental and analytical study conducted to investigate the effect of flow holes on the vibration characteristics of the LMFBR structure. In the experimental study, a simplified scale model of the LMFBR structure was used. The applicability of the vibration analysis method to the LMFBR structure was verified by comparing with the experimental data.

1. INTRODUCTION

Experimental and analytical work has been performed to study the fluid-structure interaction in a Japanese demonstration LMFBR structure. The fluid effect on seismic response of the reactor vessel and internal components are of great importance in the seismic design of LMFBRs, because the reactor vessel is a large shell structure with a thin wall, and filled with a large volume of liquid sodium. The liquid sodium in the reactor vessel is divided into two domains by a core support structure. One is an upper plenum domain with free surface and the other is a lower plenum domain closed. These domains are connected by small flow holes in the core support structure. As a result, the bottom of the reactor vessel and the core support structure contained the core structure have two resonant coupling vibration modes caused by fluid-structure interaction in the vertical direction. [1][2]

This study was performed to investigate the effect of flow holes on the vertical vibration characteristics for the LMFBR, using a simplified scale model of the LMFBR structure. First, Vibration excitation tests were carried out using a large earthquake simulator to clarify the effect of the flow holes. Secondly, Finite element analyses were performed to evaluate and verify the analytical methods, by a comparison with the experimental data.

2. SCALE MODEL

The scale model was simplified as far as possible to simulate the actual coupling vibration modes between the bottom of the reactor vessel and the core

support structure caused by the fluid-structure interaction. The scale model, which scale is one tenth, consists of a reactor vessel, a core support structure, and a core structure. Two scale models having different core shapes, as shown in Fig.1 and Fig.2, were used in the vibration tests. One is a three-dimensional structure model (Type A) with four or eight flow holes located at the core support structure, and the other is an axisymmetric structure model (Type B) with one flow hole located at the center of the core. In both models, the cylindrical vessel's diameter, height, and thickness are about 1.0 m, 1.4 m and 8.0 mm, respectively. The cylindrical section of the models is made of polyvinyl chloride resin. The bottom plate is of aluminum alloy and the others are steel. Water was substituted for the liquid sodium in the vessel. The vessel was suspended from a rigid test frame by being bolted to the frame at the top flange.

Table.1 and Fig.3 show the test cases and the flow hole geometry. For the scale model, flow hole shape was simplified as narrow circular hole, and the location and geometry of the flow holes were determined so as to simulate the actual flow holes. For the three-dimensional structure model (Type A), the case A-0 is the test without the flow hole, the other cases are the test with the flow holes in which the ratios of D to L are same considering the similarity of each flow hole shapes. In the axisymmetric structure model (Type B), the case B-0 is the test without the flow hole, the other cases are the tests with the flow holes in which the ratios of D to L are same in the case B-1,2,3 considering the similarity of each flow hole shape, and D is fixed at 18.0 mm to investigate the effect of L in the case B-1,4,5,6.

3. EXPERIMENTS AND ANALYSIS ON VIBRATION CHARACTERISTICS

Vertical vibration tests of the scale model were carried out using a large earthquake simulator. Resonant vibration modes and frequencies of the scale model were evaluated by sinusoidal wave sweep tests and wire cutting tests. The dynamic response of the model was measured by accelerometers and pressure gauges.

Figure 4 shows the resonance curve of the core vertical response acceleration against the sinusoidal wave input. In this case, two vibration modes were observed in the test frequency range. The resonant 1st (out-of-phase) mode and the 2nd (in-phase) mode were the coupling vibration modes between the core support structure and the bottom plate. The out-of-phase mode response was much smaller than the in-phase mode response for the all test cases with flow hole. Figures 5 and 6 show the relations between the resonant frequency of the coupled modes and the ratio of the total cross sectional area (A_f) of flow holes to cross sectional area (A_0) of cylindrical vessel. These results show that the out-of-phase mode frequency decreases with the flow hole area. However, the in-phase mode frequency was independent of the flow hole size and was also equal to that of the case without flow hole. Figure 7 shows the relation between the out-of-phase resonant frequency (f_0) to the power minus two and the flow hole length L in the case of the axisymmetric structure model test in which the flow hole diameters were fixed at 18 mm. This result indicates that the fluid added mass increases linearly with the flow hole length L, since the resonant frequency (f_0) to the power minus two is assumed to be approximately proportional to the fluid added mass. To clarify the effect of excitation input level on the response characteristic, sinusoidal wave sweep tests were performed, and then compared between the several inputs, as shown in Figs.8 and 9. In the out-of-phase mode, response rate of the pressure for the lower plenum to input acceleration decreased with the increase of the input acceleration. However, resonant frequency was independent of the input. In the in-phase mode, response curves for the core were independent of the input. The dependence of damping ratio on the response amplitude in the both coupled modes are shown in Figs.10 and 11. In the out-of-phase, damping ratio increased linearly with the response pressure of lower plenum which is proportional to the response acceleration of the core. In

addition, the damping ratio increased with the decrease of the flow hole area. It can be considered that this damping effect is caused by the fluid damping, which is proportional to the flow velocity squared, in the flow holes. This fluid damping force suppress the vibration response of the out-of-phase mode. In the in-phase mode, the damping ratio was independent of the response acceleration of the core.

Finite element analyses were performed to evaluate and verify the analytical methods using the analysis Codes FINAS and NASTRAN. Figure 12 and 13 show the finite element models for FINAS and NASTRAN respectively. The fluid inertial effects were taken into account using the continuum fluid elements in FINAS, the virtual mass method in NASTRAN. For the structure of the models, shell element was used. In the finite element models, a locally reduced mesh size was used for an accurate modeling of the flow hole. In order to confirm the applicability of the vibration analysis methods, the resonant frequencies and vibration modes of the scale model were compared between experimental results and analytical results, as shown in Table 2, Fig.14 and 15. The analytical results obtained by the FINAS and NASTRAN models agreed well with experimental results. In addition, participation factors obtained by the analyses indicate that the dominant mode under vertical excitation is the in-phase mode, and this is also confirmed by the response characteristics in the vertical vibration tests.

4. CONCLUSIONS

Experimental and analytical studies clarified the effect of the flow hole on the vertical vibration characteristics of the LMFBR structure. The conclusions are as follows.

- (1) The out-of-phase and in-phase vibration mode between the core support structure and the bottom plate was obtained under vertical excitation, due to the effect of the fluid communication created by the flow hole.
- (2) The out-of-phase mode frequency is decreased in keeping with the flow hole area and with the increase of the flow hole length, due to the increase in the fluid added mass.
- (3) In the case of this actual LMFBR design, the out-of-phase mode response can be ignored, since the out-of-phase mode response was much smaller than in-phase mode response under the vertical excitation.
- (4) The vibration characteristics of the in-phase mode, which was the predominant mode, were independent of the flow hole.
- (5) Analytical results considering the fluid interaction effects of the flow hole agreed well with the experimental results.
- (6) From these results, the validity of the analytical methods for the LMFBR was verified.

ACKNOWLEDGMENTS

The study has been performed as a part of joint research and development projects for DFBR, under sponsorship of the 9 Japanese electric power companies and Electric Power Development Co., Ltd.

REFERENCES

1. Sakurai A., et al. 1985. Fluid-Coupled Vibration Analysis of Reduced Models of Pool-Type LMFBR. SMiRT 8, Vol.E : pp.333-338.
2. Cheron P., et al. 1985. Detailed Representation of Fluid Structure Interaction in Seismic Analysis. SMiRT 8, Vol.E : pp.297-302.

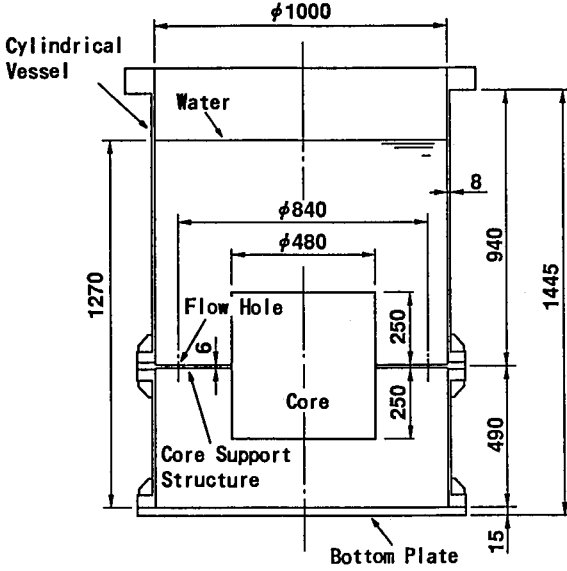


Fig. 1 1/10 scale model (Type A)

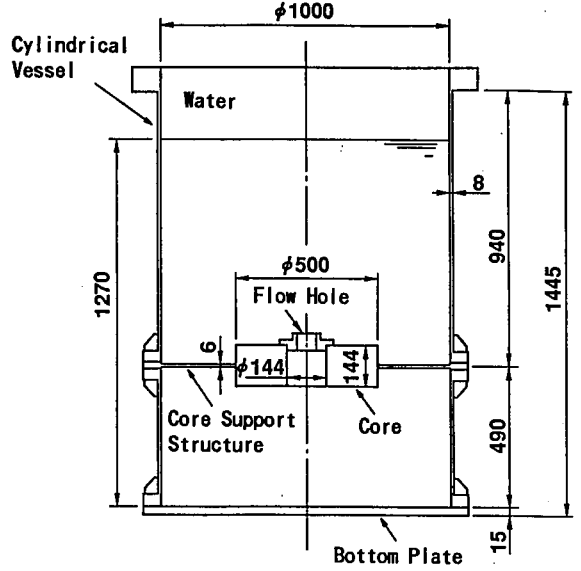


Fig. 2 1/10 scale model (Type B)

Table 1 Flow hole geometry

Model Type	Case No.	D (mm)	L (mm)	Number of Flow Holes
A	A-0	—	—	0
	A-1	9.0	9.0	4
	A-2	18.0	18.0	4
	A-3	18.0	18.0	8
B	B-0	—	—	0
	B-1	18.0	18.0	1
	B-2	36.0	36.0	1
	B-3	72.0	72.0	1
	B-4	18.0	1.8	1
	B-5	18.0	4.5	1
	B-6	18.0	72.0	1

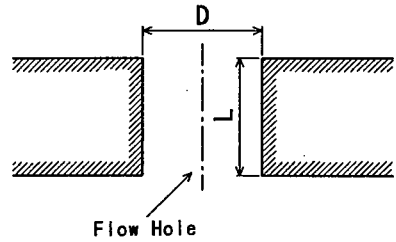


Fig. 3 Shape of flow hole

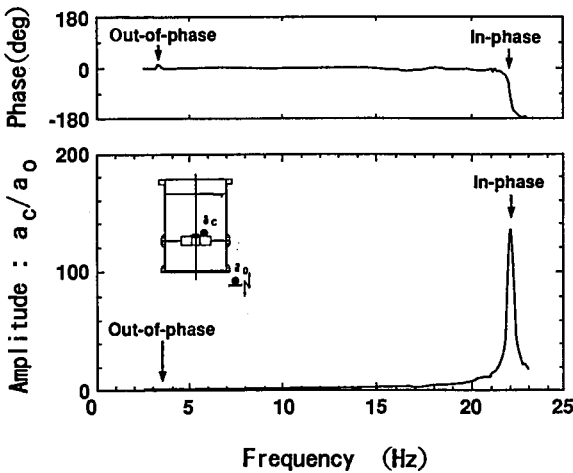


Fig. 4 Resonance curve (Case B-3)

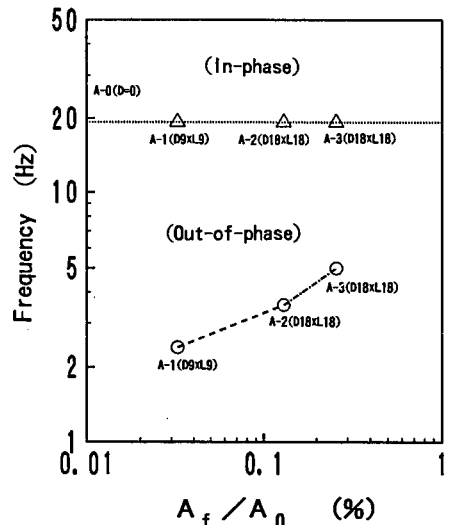


Fig. 5 Relationship between resonant frequency and area of flow hole (Type A)

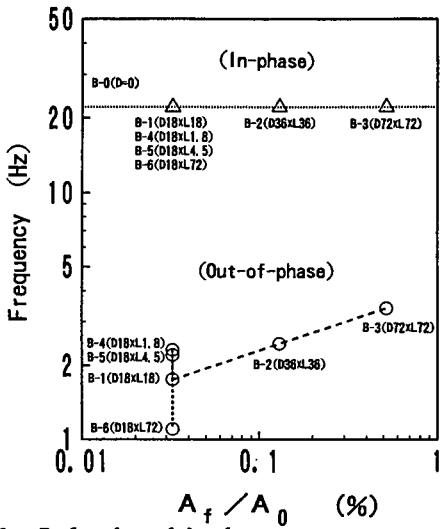


Fig. 6 Relationship between resonant frequency and area of flow hole (Type B)

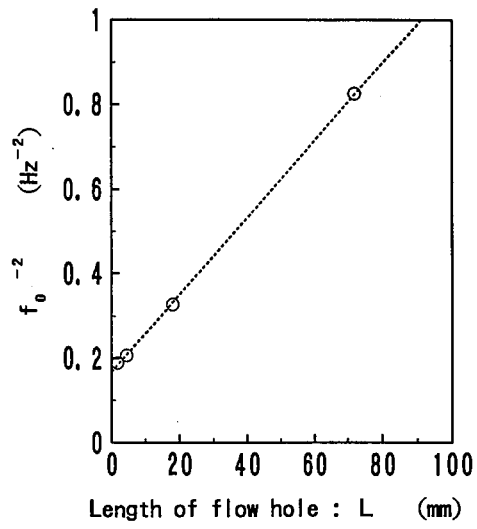


Fig. 7 Effect of flow hole length

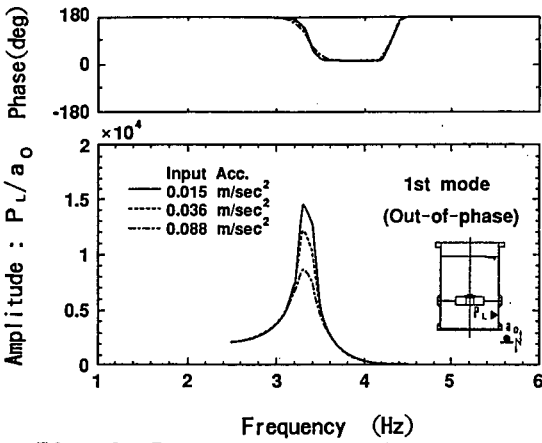


Fig. 8 Resonance curve for various input accelerations (Case B-3: out-of-phase mode)

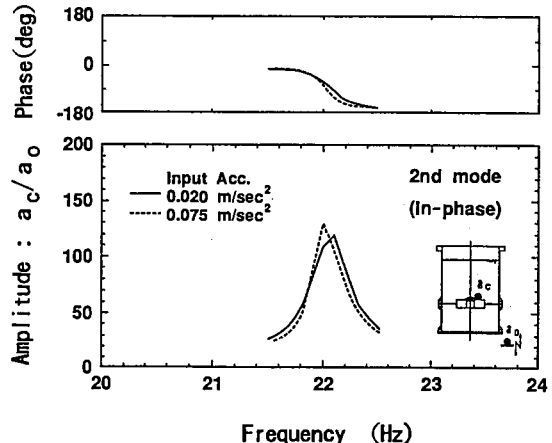


Fig. 9 Resonance curve for various input accelerations (Case B-3: in-phase mode)

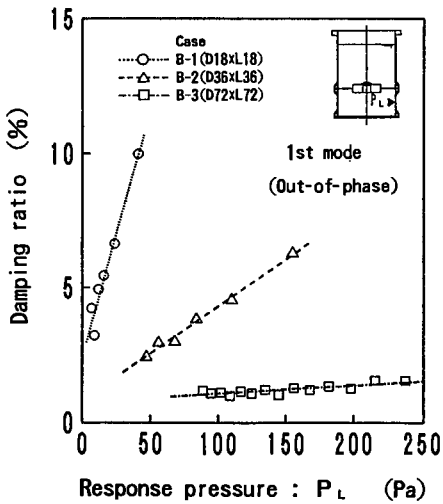


Fig. 10 Dependence of damping ratio on vibration amplitude (out-of-phase mode)

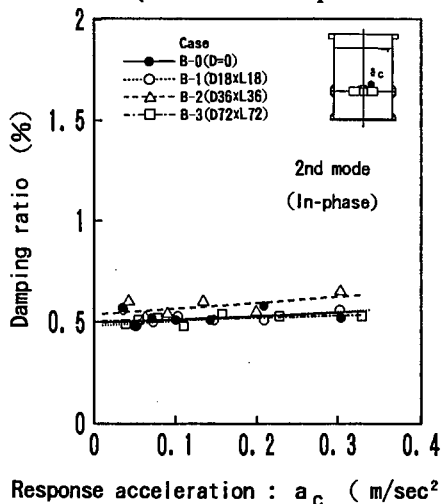


Fig. 11 Dependence of damping ratio on vibration amplitude (in-phase mode)

Table 2 Comparison between analytical results and experimental data

Case No.	Mode	Exp.	FINAS	NASTRAN
B-0 (D=0)	1st (In-phase)	22.1Hz	21.4 Hz($\beta=1.4$)	—
B-3 (D72xL72)	1st (Out-of-phase)	3.4Hz	3.0 Hz($\beta=0.03$)	3.4 Hz($\beta=0.03$)
	2nd (In-phase)	22.0Hz	21.4 Hz($\beta=1.4$)	21.9 Hz($\beta=1.6$)

β : Participation factor

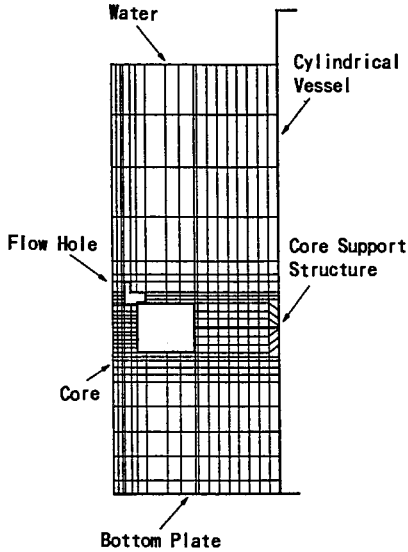


Fig. 12 FEM model (FINAS)

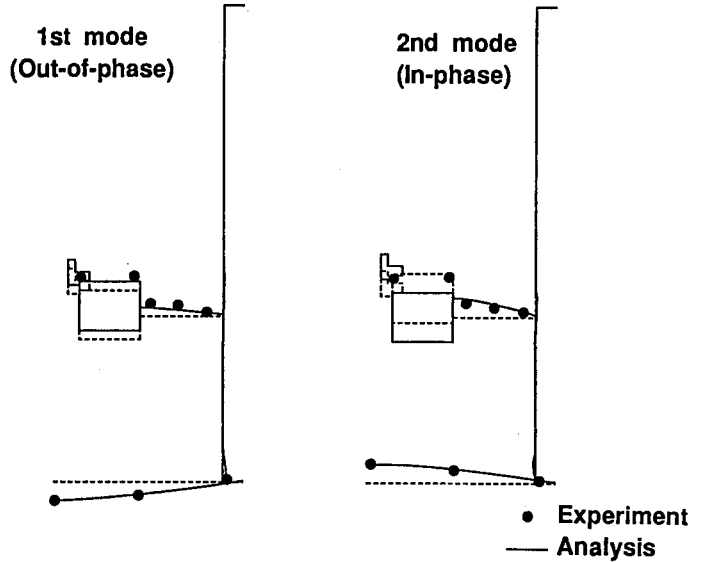


Fig. 14 Resonant vibration mode comparison between FEM (FINAS) and test results (Case B-3)

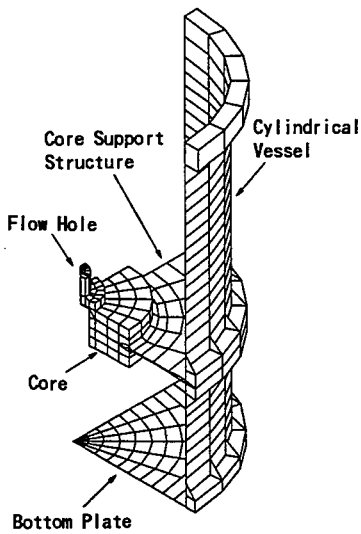


Fig. 13 FEM model (NASTRAN)

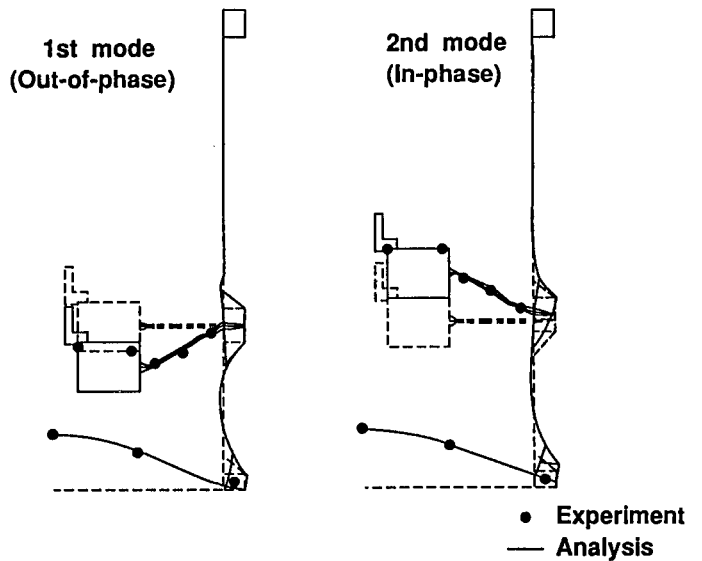


Fig. 15 Resonant vibration mode comparison between FEM (NASTRAN) and test results (Case B-3)